DOI: 10.1002/chem.200800675

The First Example of Molecularly Imprinted Nanogels with Aldolase Type I Activity

Davide Carboni,[a] Kevin Flavin,[a] Ania Servant,[a] Veronique Gouverneur,[b] and Marina Resmini*[a]

Dedicated to Professor Keith Brocklehurst on the occasion of his 70th birthday

Abstract: The molecular-imprinting approach was used to obtain a nanogel preparation capable of catalysing the cross-aldol reaction between 4-nitrobenzaldehyde and acetone. A polymerisable proline derivative was used as the functional monomer to mimic the enamine-based mechanism of aldolase type I enzymes. The diketone template used to create the cavity was designed to imitate the intermediate of the aldol reaction and was bound to the functional monomer using a reversible covalent interaction prior to polymerisation. By using a high-dilution polymerisation method, soluble imprinted nanogels were prepared with dimensions similar to those of an enzyme and with the advantage of solubility and flexibility previously unattainable with monolithic polymers. Following template removal and estimation of active-site concentrations, the kinetic characterisation of both imprinted and non-imprinted nanogels was carried out with catalyst concentrations between 0.7 and 3.5 mol%. Imprinted nanogel **AS147** was found to have a k_{cat} value of $0.25\times10^{-2}\,min^{-1}$, the highest value ever achieved with imprinted polymers catalysing C–C bond formation. Comparison of the catalytic constants for both imprinted nanogel **AS147** and non-imprinted nanogel **AS133** gave a ratio of $k_{cat\ 147}/k_{cat\ 133}=18.8$, which is indicative of good imprinting efficiency and highlights the significance of the template during the imprinting process. This work represents a significant demonstration of the superiority of nanogels, when the molecular-imprinting approach is used, over "bulk" polymers for the generation of catalysts.

Keywords: aldol reaction · enzyme catalysis · enzyme mimics · molecular imprinting · nanostructures

Introduction

The design and synthesis of catalytic systems capable of emulating enzyme activity while overcoming some of the protein's inherent limitations is a challenge that has attracted scientists for a long time. Among the different enzyme mimics studied, catalytic antibodies and imprinted polymers have shown considerable potential and led to significant results.[1] Molecular imprinting is an attractive approach for the generation of recognition sites in macromolecular systems in which a template molecule is used in a casting procedure. Valuable results have been obtained with "bulk" polymers in applications in which strong binding to the template is required, but the development of polymeric matrices with specific catalytic activity has proved to be a bigger challenge. A variety of chemical reactions have been shown to be catalysed by imprinted polymers,[2] but the rate accelerations and turnovers have been, with few exceptions,[3] disappointing. Most of the data reported in the literature concern bond breakage, in particular hydrolytic reactions with activated substrates. The only examples of catalytic C–C bond formation by imprinted polymers are a Diels–Alder condensation,[4] a Pd-catalysed cross-coupling reaction,[5] an example of class II aldolase[6] and a dimerisation by a peroxidase-like polymer.[7]

The development of catalytic microgels, first reported by Resmini et al.[8,9] and subsequently by Wulff and his group,[10] represented a significant advance in the field of

[a] D. Carboni, Dr. K. Flavin, A. Servant, Dr. M. Resmini
School of Biological and Chemical Sciences
Queen Mary, University of London
Mile End Road, London E1 4NS (UK)
Fax: (+44) 7882-3294
E-mail: m.resmini@qmul.ac.uk

[b] Dr. V. Gouverneur
Chemistry Research Laboratory
Oxford University
Mansfield Road, Oxford OX1 3A (UK)

Supporting information for this article is available on the WWW under http://www.chemeurj.org/ or from the author.

enzyme mimics. The application of the imprinting approach to flexible polymeric matrices, such as the microgels, pioneered by Wulff,[11] allowed the preparation of materials showing higher activities relative to the "bulk" polymers. This is the result of a combination of the solubility and flexibility in addition to the higher surface-to-volume ratio.

Herein we report, for the first time, the preparation of molecularly imprinted nanogels containing a proline derivative, which show high catalytic activity, turnover and enantioselectivity in the cross-aldol reaction between 4-nitrobenzaldehyde (**1**) and acetone (**2**; Scheme 1) and follow the en-

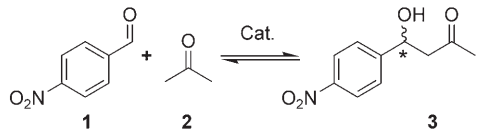

Scheme 1. Cross-aldol reaction between 4-nitrobenzaldehyde (**1**) and acetone (**2**) leading to the corresponding β-hydroxyketone **3**.

amine-based mechanism characteristic of aldolase type I enzymes. A novel method for active-site titration that involves reaction of the catalyst with a substrate and leads to formation of an easily detectable product was developed; this allowed accurate calculation of the catalytic parameters, thus providing important information on the polymer composition.

The aldol condensation is a powerful reaction in organic chemistry for the formation of C–C bonds, which gives rise to at least one new chiral centre bearing a hydroxyl group that can be further transformed. Control of the stereoselectivity of this reaction is important for its practical applications in synthesis. The use of natural aldolase or artificial enzymes, like catalytic antibodies,[12] gives important advantages, such as high stereospecificity and efficiency, but is limited by the ranges of pH, temperature and organic solvents. As part of our research in the field of enzyme mimics, and based on our extensive experience of catalytic antibodies,[13] we are focused on developing polymeric nanostructured catalysts that can mimic enzyme-like active sites. The aim of our work is not to challenge the effectiveness of enzymes and organocatalysts in their activity, enantioselectivity and substrate scope, but instead to use the imprinting technology to complement these catalysts by targeting specific products that could not be otherwise obtained. We have created a library of polymerisable amino acid derivatives that can be used alone or in combination as functional monomers in the imprinting approach. Previous examples have included the use of polymerisable arginine and tyrosine to obtain microgels for carbonate hydrolysis.[8,9]

Results and Discussion

The formation of the complex between the template and the functional monomer is a key step in molecular imprinting and its stability plays a significant role in determining the specificity of the cavities in the polymer (Scheme 2). In this work the reversible covalent approach was chosen, making use of the enol form of diketone **4** as the template and the polymerisable proline derivative **5** as the functional monomer. These two molecules react to form the corresponding enaminone **6**, which is designed to mimic the intermediate of the cross-aldol reaction. This complex contains the styrene functional group that will allow incorporation of this unit into the nanogel structure.

The proline-catalysed reaction between aldehyde **1** and acetone proceeds by a two-step mechanism. The first step involves the formation of the activated enamine **7** between the proline derivative and acetone. This subsequently reacts with **1** to give intermediate **8**, which is then hydrolysed to the final aldol product **3**. Scheme 3 shows the analogy between intermediate **8** and enaminone **6** and its resonance form **9.** Following polymerisation, acidic hydrolysis of the enaminone leads to complete cleavage of the template leaving a series of cavities containing proline-analogue groups

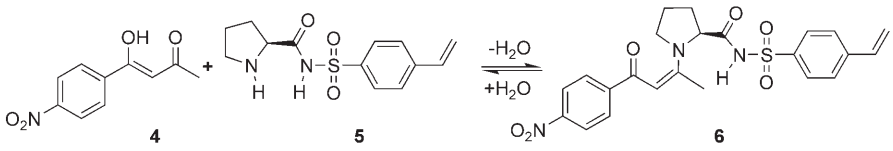

Scheme 2. Formation of the template–monomer intermediate **6** with quantitative yield in DMF at 40 °C.

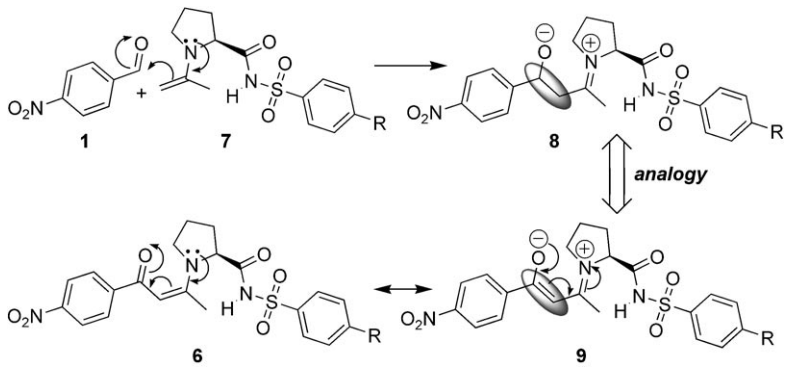

Scheme 3. Analogy between resonance structure **9** and intermediate **8** of the catalysed reaction; R = CH=CH_2 or a polymeric matrix.

located in specific positions designed to react with the acetone to form the activated enamine.

The design of functional monomer **5**, which contains a benzenesulfonamide group, was based on the structure of a successful proline analogue,[14] selected from the large pool of organocatalysts available in the literature,[15] and derivatised with a double bond that would make it suitable for polymerisation. The rationale for this work was based on the theory that the imprinting approach combined with the acidity of the sulfonamidic proton would lead to increased selectivity and catalytic activity as a result of stronger hydrogen bonding in the transition state and a more rigid environment. The choice of this molecule was determined by a combination of factors, notably the evaluation of the data available in the literature regarding small organic catalysts, the solubility and the feasibility of transforming the molecule into a polymerisable derivative.

Template **4** was synthesised from the base-catalysed aldol reaction between **1** and **2** to give a racemic mixture of **3** that was further oxidised to the diketone. The reaction of formation of enaminone **6** was monitored by thin-layer chromatography (TLC) and ^{1}H NMR spectroscopy to identify the experimental conditions leading to the complex formation with high yields. Anhydrous DMF was found to be the best solvent with complete formation of the enaminone product obtained in 48 h at 40 °C, by using activated molecular sieves under an inert atmosphere. Covalent complex **6** was isolated, purified and fully characterised by using ^{1}H, COSY and ^{13}C NMR spectroscopy and HRMS analyses. The experimental data for the ^{13}C spectra, supported by high-level NMR prediction—obtained by DFT quantum chemical calculations carried out with the parallel version of Gaussian 03[16] (see the Supporting Information)—confirmed that the nitrogen atom of proline specifically attacks the carbonyl group further away from the phenyl ring. Enaminone **6** has been shown to exist in a mixture of two geometric isomers, *E* and *Z*, in a percentage of 55:45, as evaluated from the ^{1}H NMR spectroscopic signal of the olefinic proton. The complex was shown to be stable at 70 °C, the temperature at which polymerisation occurs, and hydrolytic studies demonstrated that the reaction is completely reversible by addition of dilute HCl, therefore providing the experimental conditions for the release of the template from the nanogels after polymerisation.

The nanogels were prepared in DMF using high-dilution radical polymerisation. This technique does not use surfactants; instead stabilisation of the growing nanogels is achieved through steric control when the total monomer concentration is below the critical value, C_m, which is determined experimentally for each system.[17] Following an established protocol, acrylamide-based nanogels (with $C_m = 0.5$ and 80 % cross-linker) were synthesised with a ratio of functional monomer to acrylamide ranging from 1:1 to 1:5. After removal of the template the isolated nanogels were dissolved in DMF and DMSO to give clear colloidal solutions. For each imprinted-nanogel preparation the corresponding non-imprinted polymer (containing the proline derivative, but prepared in the absence of the template) was synthesised under identical conditions. An additional set of control polymers containing only the acrylamide and cross-linker but not the proline derivative were also prepared.

GPLC measurements were carried out on the nanogel solutions in DMSO; polymethylmethacrylate (PMMA) standards in DMSO were used to create a calibration curve. This allows a more accurate estimate of the molecular mass compared with the commonly used linear polystyrene standards. The data showed all preparations to have an average molecular mass between 258 and 288 kDa. These values are in accordance with the value of 262 kDa obtained by Wulff et al. for nanogel preparations with the same value of C_m and measured by using membrane osmometry.[10] The average particle size was measured for all of the nanogels (solutions in DMSO containing 0.5 mg mL^{-1} of polymer) by using dynamic light scattering (DLS) and was found to be between 13 and 33 nm. These data were further confirmed by using transmission electron microscopy (TEM), as illustrated in Figure 1; the particles were stained with OsO_4, a commonly used oxidant that darkens particles by oxidising the double bonds.

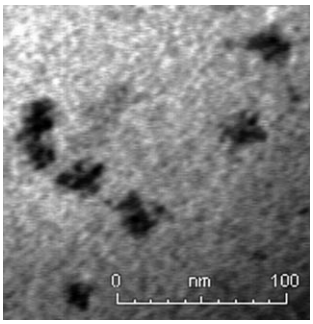

Figure 1. TEM image of imprinted nanogels showing small size distribution (scale bar: 100 nm). The particles were stained by using OsO_4 and the average diameter of the particles is ≈20 nm.

The catalytic activity of the nanogels was investigated by monitoring the formation of β-hydroxyketone **3** at $\lambda =$ 283 nm using reversed-phase HPLC. A series of experiments were carried out at fixed aldehyde and catalyst concentrations and with increasing equivalents of acetone to evaluate the dependence of the initial rate (v_i) on acetone concentration. Results showed that when using a large excess of acetone (>1300 equiv) saturation of the catalyst is achieved. This large excess of one reagent also allowed us to work under pseudo-first-order conditions, thus simplifying the kinetic studies. To verify that there is no non-specific binding of the aldehyde or the aldol product to the polymeric matrix under the reaction conditions, experiments were carried out by incubating the nanogel solutions with only the aldehyde substrate or aldol product. Results after 24 h showed that there was no change, thereby confirming that there is no alteration in initial substrate concentration and that product inhibition is not present.

Preliminary evaluation of different nanogels indicated that preparation **AS147**, containing 10% functional monomer, was the one with the highest catalytic activity and was therefore fully characterised together with the corresponding non-imprinted polymer **AS133.** Initial experiments carried out using 2.5 mg mL^{-1} of imprinted nanogel proved too fast for the HPLC monitoring protocol and initial rates could not be determined accurately. Experiments performed by varying the concentration of catalyst at constant substrate concentration showed linear dependence of the initial rate, as would be expected if catalysis were the result of the presence of the nanogels (Figure 2). From the data we chose a

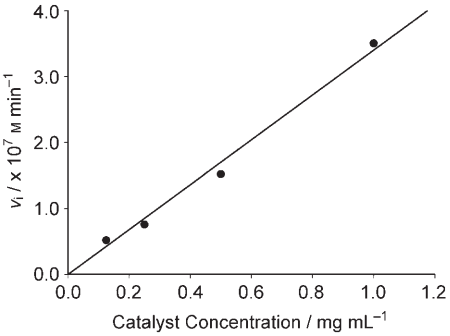

Figure 2. Graph of initial rates, v_i, versus catalyst concentration for the imprinted polymer **AS147**, for which the concentration of aldehyde was kept constant at 2 mM.

catalyst concentration (0.25 mg mL^{-1}) that, in the substrate range studied, showed good catalytic acceleration while allowing accurate kinetic parameters to be obtained.

Kinetic experiments were performed by using 0.25 mg mL^{-1} of **AS147**, **AS133** or **AS134** (20% DMSO in DMF containing 2.72 M acetone) at 25°C, and initial rates (v_i) were obtained by monitoring product **3** formation as a function of time. Figure 3 shows the data for the imprinted polymer **AS147** at different aldehyde concentrations.

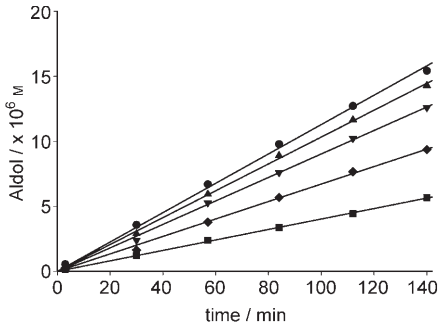

Figure 3. Determination of initial rates, v_i, for the aldol reaction between **1** and **2** catalysed by **AS147**. The graph shows formation of the aldol product **3** as a function of time with varying concentrations of **1** (■ = 2 mM, ◆ = 4 mM, ▼ = 6 mM, ▲ = 8 mM and ● = 10 mM), while the concentration of acetone is kept constant at 2.72 M. The continuous lines represent the linear regression fitting. Reactions were carried out with 0.25 mg mL^{-1} of **AS147** in a solution of 20% DMSO in DMF.

Analysis by weighted non-linear regression of the v_i versus substrate (aldehyde **1**) concentration ([S]$_0$) data shows good adherence to the Michaelis–Menten saturation model (Figure 4) and provided the values for the kinetic parameters for **AS147** of $V_{max} = 1.92 \times 10^{-7}$ (S.E. $\pm 1.58 \times 10^{-8}$) M min^{-1} (S.E. = standard error) and $K_m = 7.15 \times 10^{-3}$ (S.E. $\pm 1.14 \times 10^{-3}$) M. Comparison of the **AS147** data with the corresponding non-imprinted **AS133** data, shown in Figure 4, demonstrates a significantly higher activity for the imprinted nanogel. Kinetic data for the non-imprinted nanogel can also be fitted with a hyperbola, giving the following kinetic parameters: $V_{max} = 9.17 \times 10^{-9}$ (S.E. $\pm 5.42 \times 10^{-10}$) M min^{-1} and $K_m = 3.34 \times 10^{-3}$ (S.E. $\pm 5.48 \times 10^{-4}$) M. Both nanogel preparations contain the proline analogue and the only difference is that **AS147** was incubated with the template prior to the polymerisation. The difference in the value of V_{max} can be therefore taken as a measure of the imprinting efficiency.

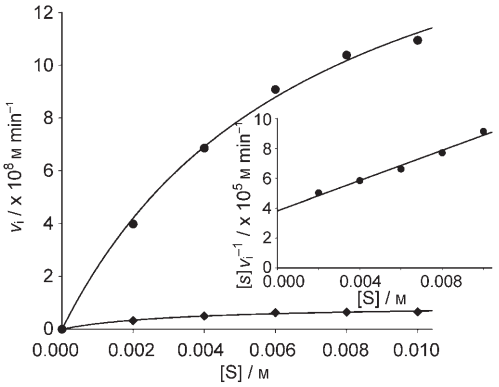

Figure 4. Adherence of the initial rates, v_i, for **AS147** (●) to the Michaelis–Menten equation is shown in comparison with the non-imprinted nanogel **AS133** (◆). Both reactions were carried out with 0.25 mg mL^{-1} of nanogel in 20% DMSO in DMF at 25°C with different concentrations of **1** ([S]). The inset graph shows the linearity of the Hanes–Woolf plot.

Imprinted polymers showing catalytic activity are often described as enzyme mimics and the kinetic parameters, k_{cat} and K_m, used in enzymology, are cited to characterise their activity. The Michaelis–Menten saturation model can be applied only if two important requirements are fulfilled: 1) the "initial" (steady-state) rate (v_i) is measured; 2) the concentration of substrate is considerably higher than the number of active sites, so that the steady-state will be promptly established, with the concentration of the catalyst–substrate complex remaining essentially constant with time and the substrate concentration approximating to its initial value.

Imprinted polymers can be described as "analogous to polyclonal antibodies", with their cavities containing a combination of different binding and catalytic sites with different characteristics. Interestingly, in our experience,[8,9] such theoretical heterogeneity appears to be contradicted by the observed functional homogeneity of the kinetic data, which do not deviate from the single-site saturation model in the substrate concentration range investigated, as evidenced by the linearity of the Hanes–Woolf plot.

As reported in the literature,[18] a mixture of catalysts with different kinetic parameters would lead to plots of [S]/v versus [S] following a markedly curved concave downwards line. Data shown in Figure 3 confirm that **AS147** is a nanogel preparation with high catalytic activity and displaying functional homogeneity.

One of the key issues in comparing different imprinted polymers is that the catalytic parameters reported are often estimates, calculated using the total functional monomer content instead of the actual concentration of active sites—the functional molarity—in the preparation.

In this work, active-site titration was achieved by treating the nanogel preparations with a solution of 4-nitrophenyl acetate (1 equiv, 55 °C, 5 d). This reagent selectively acetylates the nitrogen atom of proline, irreversibly forming the corresponding *N*-acetyl proline derivative and releasing 4-nitrophenolate, which is easily detected by using HPLC. It was found that given the low concentration of polymer used in the solutions, HPLC monitoring offered increased accuracy in the determination of the concentration of 4-nitrophenolate compared with UV-visible spectroscopy. This value corresponds to the concentration of proline units available. Results of the titration show that when using nanogel solutions of 0.25 mg mL^{-1} the following active-site concentrations are available: **AS147** = 79 μM and **AS133** = 69 μM. As expected, **AS134**, which does not contain any proline derivative, does not show any reactivity with 4-nitrophenyl acetate. These values represent 54 and 47 %, respectively, of the theoretical concentration of proline monomer in each preparation, when the corresponding yields are taken into account. The data for the imprinted nanogel **AS147** has been further confirmed by carrying out a set of rebinding experiments using template **4.** A solution of polymer (0.25 mg mL^{-1}) in 20 % DMSO in DMF with diketone **4** (1.1 equiv) was reacted for 48 h at 40 °C. HPLC measurements allowed determination of the concentration of leftover diketone, and by difference, the concentration of template that had reacted with the proline side chain contained in the nanogels. For **AS147** the value of 77 μM was obtained, which is in accordance with the data previously obtained.

It is important to note that the kinetic experiments presented in Figure 4, carried out with concentrations of **1** from 2 to 10 mM and 0.25 mg mL^{-1} of nanogel (equivalent to 77 μM active sites) clearly fulfil the requirements of the Michaelis–Menten saturation model, with the catalyst concentration ranging from 3.5 to 0.7 mol %, values that are among the lowest in the literature covering this field. The accurate value of the kinetic constant, k_{cat}, can be calculated from V_{max}/[active site] = 0.25×10^{-2} min^{-1}. This value, although still below the activity of the best aldolase enzymes, is the highest ever achieved with imprinted polymers catalysing C–C bond formation. Moreover, given that the titration experiments confirmed that both imprinted and non-imprinted nanogels contain a similar concentration of proline active sites, the large difference in rate acceleration observed between **AS147** and **AS133** can be taken as a true indication of successful imprinting. The ratio of the two catalytic constants, $k_{cat\ 147}/k_{cat\ 133} = 18.8$, provides an indication of the imprinting effect. The requirements for an efficient catalyst are 1) strong binding to the transition state and 2) weak binding to the substrate in the ground state.[19] A direct measurement of the efficiency of the imprinting strategy can be obtained by comparing the values of k_{cat}/K_m, which represent the rate constant for the overall reaction. For **AS147** $k_{cat}/K_m = 0.35$ min^{-1} M^{-1} and for **AS133** $k_{cat}/K_m = 0.04$ min^{-1} M^{-1}, which demonstrate how the imprinting strategy has led to a more efficient catalyst.

The enantioselectivity of the nanogels described in this work originates from the chirality of the functional monomer used. Experimental data confirmed that racemisation did not occur during the synthesis of the proline-containing monomer and, therefore, the enantioselectivity is expected to be retained in the polymeric matrix. To determine the enantioselectivity of the nanogels, reaction mixtures were analysed by chiral HPLC using a Diacel Chiralcel OJ-H column. The preliminary data for imprinted polymer **AS147** show an enantiomeric excess of 62 %, whereas non-imprinted polymer **AS133** gives an enantiomeric excess of 60 %. This result is not unexpected given that both nanogels contain the optically active proline derivative and that the template design was not targeting enantioselectivity. The interesting result is that the presence of the polymeric matrix and the imprinting with the template allow the enantioselectivity to be retained. A more detailed investigation of the effects of nanogel composition on the enantioselectivity will be required to further optimise these results.

Conclusion

We have successfully imprinted acrylamide-based nanogels using a covalent approach, by formation of a reversible enaminone, to obtain nanogel preparations that show remarkable catalytic activity, turnover and enantioselectivity. The low concentrations used, together with the good solubility and high imprinting efficiency make these materials a valuable alternative to biochemical catalysts. The data presented in this paper demonstrate the superiority of nanogels, when the molecular-imprinting approach is used, over "bulk" polymers for the generation of catalysts. This work represents a significant advance in the field of enzyme mimics and confirms the potential of the imprinting approach. The strategic design of the template molecule offers the invaluable opportunity to generate "ad hoc" catalysts with tailored specificities and that are able to give access to a range of molecules otherwise difficult to obtain.

Experimental Section

Instrumentation: ^{1}H (270 MHz), ^{13}C (67 MHz) and COSY NMR spectra were recorded by using a JEOL EX-270 instrument and ^{1}H (400 MHz), COSY and ^{13}C NMR (100 MHz) spectra were recorded by using a Bruker 400 MHz instrument. ^{1}H NMR peak multiplicities are reported as

follows: s (singlet), d (doublet), dd (doublet of doublet), t (triplet), q (quartet), m (multiplet). Low-resolution mass spectrometry (LRMS) data were obtained by using a reversed phase HPLC HP Agilent 1200 system combined with a Bruker Daltonics Esquire 3000 Plus mass spectrometer possessing an MSD Trap. High-resolution mass spectral data was obtained at the EPSRC National Centre, Swansea (UK) with ZQ4000 nano-electrospray. Enantiomeric excesses were measured with a Dionex P680 HPLC pump with UVD 3400 detector and using a Daicel Chiralcel OJ-H chiral column. TEM measurements were performed with a JEOL 1200 EX instrument (120 kV) with a beam at 90° on a 300 mesh copper grid.

4-Hydroxy-4-(4-nitrophenyl)butan-2-one (3): *p*-Nitrobenzaldehyde (2 g, 13.2 mmol) was dissolved in acetone (24 cm^3, 18.7 g, 322.3 mmol) in an ice bath. NaOH (2.6 cm^3, 0.613 mmol, 0.24 M) in aqueous solution was added and the mixture was stirred for 20 min. TLC analyses with petroleum ether/diethyl ether (3:7) were used to determine when the reaction was complete. The acetone was removed by rotary evaporation and the mixture was extracted three times with dichloromethane. The organic layer was dried over $MgSO_4$, filtered and concentrated under vacuum. The crude product was purified by flash chromatography (petroleum ether/diethyl ether 3:7). A whitish solid was recovered (2.12 g, 10.14 mmol, 77%). ^{1}H NMR (275 MHz, $CDCl_3$, 25°C, TMS): δ=8.19 (d, J=8.9 Hz, 2H; Ar-*H*), 7.51 (d, J=8.9 Hz, 2H; Ar-*H*), 5.26 (m, 1H; C*H*), 3.58 (d, J=3.45 Hz, 1H; O*H*), 2.84 (d, J=7.42 Hz, 2H; CH_2), 2.20 ppm (s, 3H; CH_3); ^{13}C NMR (100 MHz, $CDCl_3$, 25°C, TMS): δ=209 (*C*=O), 150 (O_2N-*C*-Ar), 147 (Ar-*C*-C-OH), 127 (Ar, 2C), 124 (Ar, 2C), 69 (Ar-*C*-OH), 52 (CH_2), 31 ppm (CH_3).

1-(4-Nitrophenyl)butane-1,3-dione (4): β-Hydroxyketone **3** (1.99 g, 9.5 mmol) was dissolved in dichloromethane (30 cm^3). Bu_4NHSO_4 (339 mg, 0.99 mmol) was subsequently added to the solution. An oxidising solution was prepared by adding $K_2Cr_2O_7$ (1.149 g, 3.90 mmol) to H_2SO_4 (35 cm^3, 30%). The oxidising mixture was added to the reaction mixture while stirring was applied. TLC analyses with petroleum ether/diethyl ether (3:7) were used to monitor the reaction and showed complete reaction after 20 min; the organic phase was then separated and the aqueous phase was extracted twice with dichloromethane. The combined organic layers were washed with saturated NH_4Cl solution and dried over $MgSO_4$, filtered and concentrated under vacuum. The crude product was purified by flash chromatography (petroleum ether/diethyl ether 3:7) and recrystallised from cold diethyl ether. A yellow solid was recovered (1.62 g, 7.82 mmol, 42%). ^{1}H NMR (275 MHz, $CDCl_3$, 25°C, TMS): δ=15.89 (s, 1H; CH=C-O*H*), 8.27 (d, J=8.9 Hz, 2H; Ar-*H*), 8.00 (d, J=8.9 Hz, 2H; Ar-*H*), 6.21 (s, 1H; CH), 2.21 ppm (s, 3H; CH_3); ^{13}C NMR (67 MHz, $CDCl_3$, 25°C, TMS): δ=196 (*C*=O), 179 (HO-*C*=CH), 150 (O_2N-*C*-Ar), 140 (Ar-*C*-C-OH), 128 (Ar, 2C), 124 (Ar, 2C), 98 (HO-C=*C*H-C=O), 26 ppm (CH_3); IR (nujol): $\tilde{\nu}$=1720 (C=O), 1219 cm^{-1} (C=C-OH); HRMS (ESI): m/z calcd for $C_{10}H_9NO_4$: 206.0459 $[M-H]^+$; found: 206.0458.

(*S*)-*N*-(4-Vinylphenylsulfonyl)pyrrolidine-2-carboxamide (5): Dicyclohexylcarbodiimide (963 mg, 4.67 mmol) was added to Fmoc-proline (1.284 g, 3.82 mmol) in dichloromethane (20 cm^3) at 0°C. After 1 h, 4-vinylbenzenesulfonamide (0.697 g, 3.80 mmol; synthesis in the Supporting Information) and dimethylaminopyridine (98 mg, 0.80 mmol) were added at 0°C. The reaction mixture was stirred for 48 h and monitored by using TLC analyses (dichloromethane/ethyl acetate 8:2). The reaction mixture was filtered, concentrated under vacuum and purified by flash chromatography (petroleum ether/ethyl acetate 6:4) to afford a white solid (0.957 g, 1.90 mmol, 50%). The solid was added to a 30% aqueous ammonia solution (30 cm^3) and homogenised with tetrahydrofuran (8 mL). The solution was allowed to react for 16 h and was extracted with diethyl ether to remove any impurity. The aqueous phase was freeze-dried for 24 h and purified by flash chromatography (dichloromethane/methanol 95:5) to afford a white solid (0.746 g, 70%). M.p. 201–206°C; ^{1}H NMR (275 MHz, $CDCl_3$+CD_3OD, 25°C, TMS): δ=7.81 (d, J=8.39 Hz, 2H; Ar-*H*), 7.39 (d, J=8.39 Hz, 2H; Ar-*H*), 6.67 (dd, J_{CIS}=10.92 Hz, J_{TRANS}=18.07 Hz, 1H; CH_2=C*H*), 5.76 (d, J_{TRANS}=18.07 Hz, 1H; CH_2=C*H*), 5.30 (d, J_{CIS}=10.92 Hz, 1H; CH_2=CH), 4.00 (m, 1H; N-C*H*-C=O), 3.28 (m, 2H; N-CH_2-CH_2), 2.23 (m, 1H; CH_2-CH_2-CHCO), 1.89 ppm (m, 1H+2H; CH_2-CH_2-CH-C=O + -CH_2-CH_2-CH-C=O); ^{13}C NMR (67 MHz, $CDCl_3$+CD_3OD, 25°C, TMS): δ=173 (-NH-CH-*C*ONH-), 142 (C_{Ar}-SO_2-), 141 (C_{Ar}-CH=CH_2), 136 (-*C*H=CH_2), 127 (Ar, 2C), 126 (Ar, 2C), 116 (-CH=*C*H_2), 62 (-NH-*C*H-CONH-), 46 (CH_2-CH_2-NH-CH-), 29 (-CH_2-NH-CH-CH_2-), 24 ppm (-CH_2-CH_2-NH-CH-); HRMS (ESI): m/z calcd for $C_{13}H_{17}O_3N_2S$: 281.0954 $[M+H]^+$; found: 281.0953.

1-(4-(4-Nitrophenyl)-4-oxobut-2-en-2-yl)-*N*-(4-vinylphenylsulfonyl)pyrrolidine-2-carboxamide (6): Compound **5** (141 mg, 0.51 mmol) dissolved in dry dimethylformamide (4 cm^3) was added to **4** (105 mg, 0.51 mmol) under a nitrogen atmosphere. Activated molecular sieves (0.4 nm) were added to the mixture, which was stirred for 64 h at 40°C. After 64 h, the reaction was shown to be complete by using TLC analyses (dichloromethane/methanol 8:2). The reaction mixture was purified by flash chromatography (dichloromethane/methanol 95:5), without any previous work up. A quantity of template–monomer complex was recovered (167 mg, 0.36 mmol, 71%). The desired compound was obtained pure as a mixture of the *E* and *Z* geometric isomers. The compounds were characterised by using ^{13}C NMR spectroscopy. The ^{1}H NMR and COSY-NMR spectra clearly confirmed the formation of the enaminone. M.p. 106°C; ^{1}H NMR ([D_6]DMSO, 400 MHz, 25°C, TMS) (mixture of *E* and *Z* isomers; see the Supporting Information): *p*-nitro-Ar: δ=8.22 (d, J=8.00 Hz, 2H; Ar-*H*), 8.01 ppm (d, J=8.00 Hz, 2H; Ar-*H*); *p*-nitro-Ar: 8.14 (d, J=8.00 Hz, 2H; Ar-*H*), 7.83 ppm (d, J=8.00 Hz, 2H; Ar-*H*); benzenesulfonamide-Ar : 7.72 (d, J=8.00 Hz, 2H; Ar-*H*), 7.53 ppm (d, J=8.00 Hz, 2H; Ar-H); benzenesulfonamide-Ar: 7.67 (d, J=8.00 Hz, 2H; Ar-*H*), 7.28 ppm (d, J=8.00 Hz, 2H; Ar-*H*); styrenic: 6.78 (dd, J_{CIS}=12.00 Hz, J_{TRANS}=16.00 Hz, 1H; CH_2=C*H*), 5.93 (d, J_{TRANS}=16.00 Hz, 1H; CH_2=CH), 5.36 ppm (d, J_{CIS}=12.00 Hz, 1H; CH_2=CH); styrenic: 6.61 (dd, J_{CIS}=12.00 Hz, J_{TRANS}=16.00 Hz, 1H; CH_2=C*H*), 5.77 (d, J_{TRANS}=16.00 Hz, 1H; CH_2=CH), 5.28 ppm (d, J_{CIS}=12.00 Hz, 1H; CH_2=CH); enaminic proton for major isomer: 5.58 ppm (s, 1H; C=O-C*H*=C-N); enaminic proton for minor isomer: 5.43 ppm (s, 1H; C=O-C*H*=C-N); COSY-NMR ([D_6]DMSO, 400 MHz, 25°C, TMS) (mixture of *E* and *Z* isomers; see the Supporting Information); ^{13}C NMR ([D_6]DMSO, 67 MHz, 25°C, TMS) (mixture of *E* and *Z* isomers): δ=(183.31/183.02), (175.45/175.12), (163.27/162.82), (148.89/148.60), 144.34, (128.63, 127.53, 126.16, 126.05, 123.85, 123.68), 116.74, (93.05/92.33), (65.31/64.87), (50.00/49.62), (31.09/30.89), (23.75/23.20), 17.87 ppm (see the Supporting Information); HRMS (ESI): m/z calcd for $C_{23}H_{24}O_6N_3S$: 470.1380 $[M+H]^+$; found: 470.1378.

Preparation of the imprinted nanogels: The synthesis of the template–monomer complex was performed in situ under an N_2 atmosphere at 40°C in a crimp cap Wheaton vial for 48 h. Following the addition of a mixture of *N,N′*-methylenebisacrylamide, acrylamide and azobisisobutyronitrile in DMF the polymerisation mixture—with C_m=0.5, 80% cross-linker and a ratio of catalytic monomer/acrylamide of either 1:1 (**AS147**, **AS133**, **AS134**) or 1:5 (**AS141**, **AS142**, **AS143**)—was put into an oven at 70°C. After removal of the template, the isolated nanogels were analysed to assess their solubility and it was shown to be good in DMSO, DMF or a mixture of both. Each polymer preparation imprinted with the template was complemented by the corresponding non-imprinted polymer and a control polymer that did not contain functional monomer. The characterisation of the nanogel particles were performed by using different techniques that included DLS, with solutions containing 0.5 mg cm^{-3} of nanogel in DMSO, gel permeation liquid chromatography (GPLC) using a calibration curve obtained with PMMA and finally with TEM. The particles were stained with OsO_4, a strong oxidant widely used to darken particles by oxidising the double bonds. All of the data obtained show that the average particle size measures approximately 20 nm, with a very low dispersity, and with an average molecular weight of 260 kDa.

Active-site titration: Solutions of polymer (4.5 mg cm^{-3}) were prepared in 20% DMSO in DMF (using **AS147** (18.3 mg), **AS133** (18.3 mg) and **AS134** (18.1 mg) dissolved in anhydrous DMF (2.8 cm^3) and anhydrous DMSO (0.8 cm^3) in three different vials). A solution of 4-nitrophenylacetate (0.4 cm^3, 26.46 mM) in DMF was added at t=0 min to the polymer solutions to obtain a final concentration of 2.646 mM. As a reference, a 2.646 mM solution of 4-nitrophenylacetate on its own and a 2.646 mM solution of 4-nitrophenylacetate in the presence of proline benzenesulfona-

mide were also monitored. All solutions were heated to 55 °C for 5 d and UV/Vis scans of the solutions were taken at $t=0$ min. The concentration of product formed was determined by HPLC analyses. 200 μL of each solution was added to 10 μL of internal standard and 25 μL of this new solution was injected into the HPLC instrument. The product concentration was determined by using a calibration curve of the ratio of area of 4-nitrophenol out of area of internal standard (methyl-4-nitrobenzoate).

General procedure for the kinetic measurements: To evaluate the kinetic profile of aldehyde **1** reacting with ketone **2** at 25 °C, the reaction mixture was prepared with 60 % v/v DMF, 20 % v/v DMSO and 20 % v/v acetone. The concentration of the nanogel in the reaction mixture was kept constant at 0.25 mg cm^{-3} and the final concentration of the acceptor aldehyde in the reaction mixture varied from 2 to 10 mM. Reactions were initiated by addition of 4-nitrobenzaldehyde to the nanogel solution. Initial velocities were determined by monitoring product formation by using HPLC analyses within <5 % reaction completion. The points were determined experimentally and the best-fit value of V_{max} and K_m were obtained by fitting the v_i versus $[S]_0$ data to hyperbolic saturation curves by weighted non-linear regression using Sigmaplot 8.0 (from SPSS Inc.).[20]

Acknowledgements

We thank Dr. Sarah Lee (Oxford) for her help with the HPLC enantioselectivity measurements. This work was supported by GlaxoSmithKline and Queen Mary (studentship to D.C.) and by the EC by means of the Marie Curie RTN NASCENT (MRTN-CT-2006-033873, for A.S. and K.F.).

[1] For a review see: a) A. J. Kirby, *Angew. Chem.* **1996**, *108*, 770–790; *Angew. Chem. Int. Ed. Engl.* **1996**, *35*, 706–724; b) G. Wulff, *Chem. Rev.* **2002**, *102*, 1–27; c) M. E. Davis, A. Katz, W. R. Ahmad, *Chem. Mater.* **1996**, *8*, 1820–1839.

[2] C. Alexander, H. S. Andersson, L. I. Andersson, R. J. Ansell, N. Kirsch, I. A. Nicholls, J. O'Mahony, M. J. Whitcombe, *J. Mol. Recognit.* **2006**, *19*, 106–180.

[3] J. Q. Liu, G. Wulff, *Angew. Chem.* **2004**, *116*, 1307–1311; *Angew. Chem. Int. Ed.* **2004**, *43*, 1287–1290.

[4] a) S. C. Liu, K. Mosbach, *Macromol. Rapid Commun.* **1997**, *18*, 609–615; b) D. A. Visnjevski, R. Schomäcker, E. Yilmaz, O. Brüggemann, *Catal. Commun.* **2005**, *6*, 601–606.

[5] A. N. Cammidge, N. J. Baines, R. K. Bellingham, *Chem. Commun.* **2001**, 2588–2589.

[6] a) J. Matsui, I. A. Nicholls, I. Karube, K. Mosbach, *J. Org. Chem.* **1996**, *61*, 5414–5417; b) I. A. Nicholls, J. Matsui, M. Krook, K. Mosbach, *J. Mol. Recognit.* **1996**, *9*, 652–657; c) J. Hedin-Dahlström, J. P. Rosengren-Holmberg, S. Legrand, S. Wikman, I. A. Nicholls, *J. Org. Chem.* **2006**, *71*, 4845–4853.

[7] Z. Y. Cheng, L. W. Zhang, Y. Z. Li, *Chem. Eur. J.* **2004**, *10*, 3555–3561.

[8] S. Maddock, P. Pasetto, M. Resmini, *Chem. Commun.* **2004**, 536–537.

[9] P. Pasetto, S. C. Maddock, M. Resmini, *Anal. Chim. Acta* **2005**, *542*, 66–75.

[10] G. Wulff, B.-O. Chong, U. Kolb, *Angew. Chem.* **2006**, *118*, 3021–3024; *Angew. Chem. Int. Ed.* **2006**, *45*, 2955–2958.

[11] A. Biffis, N. B. Graham, G. Siedlaczek, S. Stalberg, G. Wulff, *Macromol. Chem. Phys.* **2001**, *202*, 163–171.

[12] R. A. Wagner, R. Lerner, C. F. Barbas III, *Science* **1995**, *270*, 1797.

[13] a) V. Maggiotti, M. Resmini, V. Gouverneur, *Angew. Chem.* **2002**, *114*, 1054–1056; *Angew. Chem. Int. Ed.* **2002**, *41*, 1012–1014; b) G. Boucher, B. Said, L. Ostler, M. Resmini, K. Brocklehurst, G. Gallacher, *Biochem. J.* **2007**, *401*, 721–726.

[14] a) A. Berkessel, B. Koch, J. Lex, *Adv. Synth. Catal.* **2004**, *346*, 1141–1146; b) A. J. A. Cobb, D. M. Shaw, D. A. Longbottom, J. B. Gold, S. V. Ley, *Org. Biomol. Chem.* **2005**, *3*, 84–96.

[15] a) B. List, R. Lerner, C. F. Barbas III, *J. Am. Chem. Soc.* **2000**, *122*, 10, 2395–2396; b) K. Sakthivel, W. Notz, T. Bui, C. F. Barbas III, *J. Am. Chem. Soc.* **2001**, *123*, 5260–5267; c) B. List, P. Pojarliev, C. Castello, *Org. Lett.* **2001**, *3*, 573–575; for a review see: d) P. Dalko, L. Moisan, *Angew. Chem.* **2004**, *116*, 5248–5286; *Angew. Chem. Int. Ed.* **2004**, *43*, 5138–5175; e) H. Pellissier, *Tetrahedron* **2007**, *63*, 9267–9331.

[16] Gaussian 03, Revision C.02, M. J. Frisch, G. W. Trucks, H. B. Schlegel, G. E. Scuseria, M. A. Robb, J. R. Cheeseman, J. A. Montgomery, Jr., T. Vreven, K. N. Kudin, J. C. Burant, J. M. Millam, S. S. Iyengar, J. Tomasi, V. Barone, B. Mennucci, M. Cossi, G. Scalmani, N. Rega, G. A. Petersson, H. Nakatsuji, M. Hada, M. Ehara, K. Toyota, R. Fukuda, J. Hasegawa, M. Ishida, T. Nakajima, Y. Honda, O. Kitao, H. Nakai, M. Klene, X. Li, J. E. Knox, H. P. Hratchian, J. B. Cross, V. Bakken, C. Adamo, J. Jaramillo, R. Gomperts, R. E. Stratmann, O. Yazyev, A. J. Austin, R. Cammi, C. Pomelli, J. W. Ochterski, P. Y. Ayala, K. Morokuma, G. A. Voth, P. Salvador, J. J. Dannenberg, V. G. Zakrzewski, S. Dapprich, A. D. Daniels, M. C. Strain, O. Farkas, D. K. Malick, A. D. Rabuck, K. Raghavachari, J. B. Foresman, J. V. Ortiz, Q. Cui, A. G. Baboul, S. Clifford, J. Cioslowski, B. B. Stefanov, G. Liu, A. Liashenko, P. Piskorz, I. Komaromi, R. L. Martin, D. J. Fox, T. Keith, M. A. Al-Laham, C. Y. Peng, A. Nanayakkara, M. Challacombe, P. M. W. Gill, B. Johnson, W. Chen, M. W. Wong, C. Gonzalez, J. A. Pople, Gaussian, Inc., Wallingford CT, **2004**.

[17] N. B. Graham, J. Mao, *Colloids Surf. A* **1996**, *118*, 211–220.

[18] C. W. Wharton, A. Cornish-Bowden, K. Brocklehurst, E. M. Crook, *Biochem. J.* **1974**, *141*, 365–381.

[19] A. Fersht, *Structure and Mechanism in Protein Science: A Guide to Enzyme Catalysis and Protein Folding*, Freeman, New York, **1999**, pp. 362–365.

[20] Sigmaplot 8.0, SPSS Inc., California, **1986–2001**.

Received: April 9, 2008
Published online: July 4, 2008

